Nucleosynthesis driven by Coulomb explosion within a single nanodroplet

Isidore Last and Joshua Jortner
School of Chemistry, Tel-Aviv University, Ramat Aviv, 69978 Tel-Aviv, Israel
(Received 19 December 2007; revised manuscript received 17 January 2008; published 4 March 2008)

We demonstrate that fusion and nucleosynthesis reactions between light and heavy nuclei driven by Coulomb explosion (CE) of nanodroplets will be dominated by intrananostructure collisions within a single, large heteronuclear nanodroplet (with initial radii of $R_0=1000-3000$ Å) in ultraintense, near-infrared laser fields (peak intensities of $I_M=10^{20}-10^{21}$ W cm^{-2}). A computational and theoretical study of the yields of the intrananodroplet ^{3}T$(d,n)^4$He fusion and ^{12}C$(p,\gamma)^{13}$N nucleosynthesis reactions driven by CE of $(D^+T^+)_n$ and $(C^{6+}H_4^+)_n$ heteronuclear nanodroplets provides a manifestation of kinematic overrun effects. The ^{3}T$(d,n)^4$He fusion yield of $Y_{\mathrm{INTRA}}\simeq 200$ per nanodroplet per laser pulse within a $(DT)_n$ nanodroplet ($n=2\times10^9$, $R_0=2700$ Å) is sufficiently high to warrant experimental observation for a single nanodroplet. The ^{12}C(p,γ) ^{13}N reaction yield within a $(CH_4)_n$ nanodroplet ($n=3.9\times10^8$; $R_0=1790$ Å) is $Y_{\mathrm{INTRA}}\simeq 4\times10^{-4}\gamma$ rays per nanodroplet per laser pulse, so that this intrananodroplet nucleosynthesis is amenable to experimental observation only in an assembly of such nanodroplets. A striking manifestation is provided for the absence of kinematic overrun effects in CE of $(C^{6+}D_4^+)_n$ nanodroplets (with a kinematic parameter $\eta_{\mathrm{DC}}=1$), where intrananodroplet $D^+ + C^{6+}$ collisions and the ^{12}C$(d,n)^{13}$N reaction are precluded. CE driven intrananodroplet nuclear reaction involves transient temporal confinement of the heavy nuclei on the 10–20 fs time scale, with the heavy nuclei subcluster acting as a target for the expanding light protons or deuterons.

DOI: 10.1103/PhysRevA.77.033201 PACS number(s): 36.40.Qv, 25.60.Pj, 34.10.+x

I. INTRODUCTION

Clusters and nanodroplets (CaNs) interacting with ultraintense and ultrashort near-infrared laser pulses (peak intensities $I_M=10^{15}-10^{21}$ W cm^{-2} and pulse duration $\tau=10-100$ fs) undergo extreme ionization [1–3] with the production of ultrahigh charges, e.g., completely ionized D_2O, CH_4, and CD_4 molecules [4–7] or Xe^{q+} ($q=26-36$) ions [8–11], and attain ultrahigh energies (keV–MeV) of ions and nuclei in Coulomb explosion (CE). CE of deuterium-containing CaNs in a cluster beam [4–6,12] or a nanodroplet spray [7,13,14] produced deuterons in the energy range of 5 keV–1.5 MeV, which drive the ^{2}D$(d,n)^3$He and ^{2}D$(d,p)^3$T *dd* fusion reactions. Also amenable to experimental observation will be the nucleosynthesis reactions ^{12}C$(p,\gamma)^{13}$N, ^{14}N$(p,\gamma)^{15}$O, and ^{16}O$(p,\gamma)^{17}$F driven by ultrahigh-energy (i.e., 10–30 MeV for the heavy nuclei and 1–3 MeV for the protons) CE of $(CH_4)_n$, $(NH_3)_n$, and $(H_2O)_n$ nanodroplets [15,16]. Here and henceforth we refer to spherical nanostructures with an initial radius of $R_0\geq 100$ Å (10 nm) as nanodroplets, while such nanostructures with $R_0<100$ Å will be referred to as clusters. High-energy CE of CaNs transcends molecular dynamics toward nuclear reactions, with the realization of effective targets for tabletop *dd* fusion [4–7,12,14] and for nucleosynthesis involving heavier nuclei, which are of astrophysical interest [15,16].

Studies of the mechanisms, yields, and temporal resolutions for particle (neutrons or γ-rays) emission for nuclear reactions driven by CE of CaNs focused on inter-CaN (INTER) reactions, which occur between nuclei produced from different CaNs [3–7,12–18]. Fusion and nucleosynthesis reactions can also be generated by collisions between nuclei (or ions) within a single exploding CaN. A mechanism for intra-CaN (INTRA) collisions between light and heavy nuclei (ions) involves kinematic overrun effects in the nonuniform CE of heteronuclear CaNs, e.g., $(D_2^+O^{8+})_n$, $(C^{6+}H_4^+)_n$, $(H^+I^{25+})_n$, and $(D^+I^{25+})_n$, when the light nuclei (ions) overrun the heavy nuclei (ions) [17–19]. An experimental confirmation [4–6] of our theoretical predictions [17,18] for kinematic overrun effects was provided in CE of $(CH_4)_n$ and $(CD_4)_n$ heteroclusters. The possibility of collisions between identical nuclei during CE of a single homonuclear CaN, e.g., $(D_2)_n$, was addressed by Kaplan *et al.* [20] who found that CE of such CaNs with nonuniform density profiles caused ion overrun effects, with the formation of multiple ion flows, which were referred to as shock shells [20] that could drive collisions between identical ions. Peano *et al.* [21,22] proposed that nonuniform density profiles resulting in the formation of pronounced shock shells in homonuclear CaNs can be induced by a two-pulse irradiation scheme, so that, in the case of large $(D_2)_n$ clusters, an intracluster reaction may be attained [22]. It is still an open question whether shock wave phenomena originating from density spikes in CE of homonuclear clusters with a nonuniform density profile [20] can be realized, since even in the case of extremely narrow shell widths there is no compression of matter and the interparticle distances continue to grow smoothly [19]. Irrespective of shock wave phenomena, thin shell formation of the expanding light ions, e.g., D^+, due to kinematic overrun effects prevails in CE of heteronuclear CaNs [19,23]. Collisions within thin shells of deuterons may drive *dd* fusion in CE of both homonuclear deuterium CaNs [20–22] and of heteronuclear deuterium containing CaNs [23]. There is another important difference between INTRA reactions in CE of a homonuclear CaN and of a heteronuclear CaN. In the former case collisions between identical nuclei (ions) occur only within the thin shells, whereas in the latter case collisions between light and heavy nuclei (ions) occur throughout the entire volume of the exploding CaN.

In this paper, we advance and analyze INTRA fusion and nucleosynthesis that involve reactions between light and

heavy nuclei driven by CE within a single heteronuclear CaN. Our work provides an application of kinematic effects for the dynamics of INTRA reactions. On the basis of theoretical-computational studies we show that the attainment of efficient INTRA reactions requires the use of the large, completely ionized, heteronuclear nanodroplet (with masses and charges of nuclei satisfying constraints imposed by kinematic parameter effects [17,19]) to drive high-energy collisions between nuclei in nonuniform CE. The INTRA nuclear reactions between different nuclei are generated over the entire volume of the exploding heteronuclear CaN during the early temporal stages of CE, when the density of the nuclei is large.

II. MECHANISM AND YIELDS FOR INTRA-CaN REACTIONS

INTRA collisions and reactions in a heteronuclear CaN may be induced by three mechanisms. (i) The contribution from the exploding surface profile. This effect is small for an ordinary initial surface profile of elemental and molecular CaNs [22]. (ii) Anisotropy in the time-dependent spatial distribution of the ions, which originates from the driving of the ions by nanoplasma electrons. CE is isotropic under the initial conditions of cluster vertical ionization (CVI) [24], when outer ionization is complete in the initial, spherically symmetric, nanodroplet nuclear configuration of the CaN [17,19,25]. (iii) Kinematic overrun processes [17–19]. This mechanism is exclusive when CE preserves spherical symmetry and dominates [see point (ii)] for INTRA reactions in nanodroplets. Mechanism (iii) is realized when, in the course of CE, the inner ions attain a higher velocity than the ions on the outer periphery. In an initially homogeneous and spherically symmetric nanodroplet, the (lighter) ion i with mass m_i and charge q_i will overrun the (heavier) ion j with mass m_j and charge q_j, provided that the kinematic parameter (which is obtained under CVI conditions), $\eta_{ij}=q_i m_j/q_j m_i$, is larger than unity [17]. We shall now study INTRA reactions induced by overrun effects in CE of $(D^+T^+)_n$ nanodroplets with $\eta_{DT}=1.5$, and$(C^{6+}H_4^+)_n$ nanodroplets with $\eta_{HC}=2$. In the $(TD)_n$ nanodroplet the deuterons overrun the tritons, facilitating the $^3T(d,n)^4He$ fusion reaction, while in the $(C^{6+}H_4^+)_n$ cluster the protons overrun the carbon nuclei, facilitating the nucleosynthesis $^{12}C(p,\gamma)^{13}N$ reaction. As a counterexample we note that CE of $(C^{6+}D_4^+)_n$ nanodroplets will not generate the INTRA $^{12}C(d,n)^{13}N$ reaction as its kinematic parameter is $\eta_{DC}=1$.

Consider a molecular heteronanodroplet $(A_{k_A}B_{k_B})_n$ consisting of light A atoms and heavy B atom, with $\eta_{AB}>1$. The CaN is initially spherically symmetric, and it will be assumed that CE does not violate spherical symmetry. This picture is applicable for CE under CVI conditions [see point (ii) above]. The time-dependent differential yield for the $A+B$ INTRA reaction is then

$$y(t)=4\pi\int_0^{R_B(t)} r^2\rho_A(r,t)\rho_B(r,t)\langle\sigma v\rangle dr, \tag{1}$$

where $R_B(t)$ is the time-dependent boundary radius for the spatial distribution of the heavy ions, $\rho_A(r,t')$ and $\rho_B(r,t)$ are the local, time-dependent ion densities, and $\langle\sigma v\rangle$ is the product of the reaction cross sections $\sigma(E')$ and the center of mass collision velocity v averaged over the center of mass energy E' distribution. $\langle\sigma v\rangle$ is determined by

$$\langle\sigma v\rangle=\int_0^\infty \mathrm{P}(E';r,t)\sigma(E')v(E')dE', \tag{2}$$

with $P(E';r,t)$ being the distribution function of the center of mass energy E'. The center of mass energy E' and the velocity v are expressed by the laboratory frame energies E_A and E_B

$$E'=\mu_{AB}[(E_A/m_A)^{1/2}-(E_B/m_B)^{1/2}]^2, \tag{3}$$

$$v=(2E_A/m_A)^{1/2}-(2E_B/m_B)^{1/2}, \tag{4}$$

where m_A and m_B are the ion masses and μ_{AB} is the reduced mass. The center of mass energy E' distribution

$$P(E';r,t)=\int_0^{(E_A)_M} P_A(E_A;r,t)P_B(E_B;r,t)dE_A \tag{5}$$

is also expressed by the laboratory frame energies, with E_B expressed by E_A and E', Eq. (3), and $(E_A)_M$ being the maximal E_A energy at point r at time t. The total yield for the INTRA reaction (per cluster and per laser pulse) is

$$Y_{\mathrm{INTRA}}=\int_{t_s}^\infty dt' y(t'), \tag{6}$$

where $y(t')$ is given by Eq. (1), and t_s is the onset time (corresponding to $t_s=0$ for the onset of CE under CVI conditions and to the onset of the laser pulse [26] for a complete simulation). In view of the isotropic, spherically symmetric CE used herein we expect that the INTRA yields, Eqs. (1)–(6), incorporate the contributions of mechanisms (i) and (iii) in a full simulation.

III. SCALED MOLECULAR DYNAMICS SIMULATIONS

The large nanoparticle sizes (containing 10^7-10^9 atoms) for which INTRA reactions occur, preclude the use of traditional, particle molecular dynamics (MD) methods. Data for the ion kinetic energy distributions $P_A(E_A;r,t)$ and $P_B(E_B;r,t)$, which determine the INTRA reaction yield [Eq. (5)], were obtained from simulations of scaled electron and ion dynamics (SEID) for nanodroplets in ultraintense laser fields [16,27,28]. The SEID considers MD in a scaled nanodroplet with a reduced number of composite particles (i.e., pseudoelectrons and pseudo ions or nuclei), scaled initial interpseudoparticle distances, and scaled short-range potential parameters [28]. A single scaling parameter s ($\gg 1$) is used for the composition, mass, and charge of all the pseudoparticles, while the initial distances between the pseudoparticles are scaled by $s^{1/3}$. Our SEID simulations for nanodroplet CE are based on standard MD simulations for the pseudoparticles [28]. The s values were chosen to guarantee the independence of the resulting energetic and dynamic parameters on s. The conditions for the accuracy of the SEID method

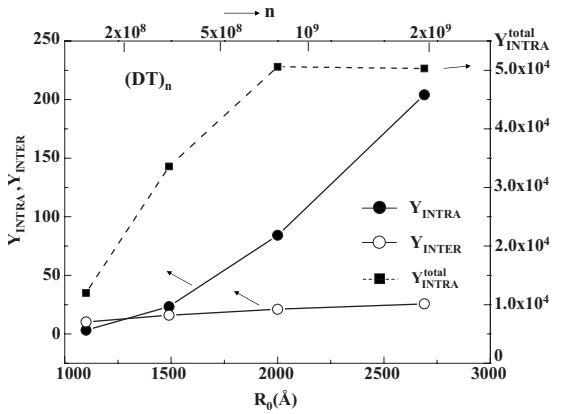

FIG. 1. Nanodroplet size dependence of the neutron yield Y_{INTRA}, Eqs. (1) and (6), for the intrananodroplet $^3\mathrm{T}(d,n)^3\mathrm{He}$ fusion driven by CE of $(\mathrm{D}^+\mathrm{T}^+)_n$ ($n=1.4\times10^8-2.0\times10^9$; $R_0=1000-2600$ Å). The total intradroplet yields $Y_{\mathrm{INTRA}}^{\mathrm{total}}$, Eqs. (7) and (8), for an assembly of nanodroplets ($V_f=5\times10^{-7}$ cm^3 and $\rho_{\mathrm{mol}}=1.0\times10^{18}$ cm^{-3}) are also given. In addition, the interdroplet yields (per nanodroplet), Y_{INTER}, Eq. (9), are presented. Calculations were performed under CVI conditions.

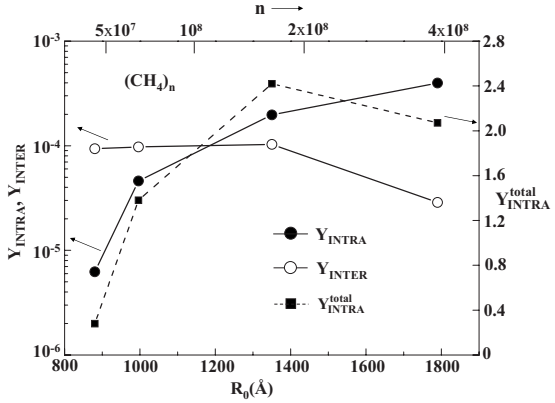

FIG. 2. Nanodroplet size dependence of γ-ray yield Y_{INTRA}, Eqs. (1) and (6), for the intrananodroplet $^{12}\mathrm{C}(p,\gamma)^{13}\mathrm{N}$ nucleosynthesis driven by CE of $(\mathrm{C}^{6+}\mathrm{H}_4^+)_n$ ($n=4.6\times10^7-3.9\times10^8$; $R_0=800-1790$ Å). The total intradroplet yields $Y_{\mathrm{INTRA}}^{\mathrm{total}}$, Eqs. (7) and (8), for an assembly of nanodroplets ($V_f=5\times10^{-7}$ cm^3; $\rho_{\mathrm{mol}}=4.0\times10^{18}$ cm^{-3}) are also given. In addition the internanodroplet yields (per nanodroplet) Y_{INTER}, Eq. (9), are presented. Calculations were performed under CVI conditions.

rest on the realization of nearly identical accelerations and trajectories of the nanodroplet particles and of the composite pseudoparticles within the scaled nanodroplet. The largest nanodroplet sizes, n_{max}, treated by us with the SEID simulations correspond to $\simeq4\times10^9$ atoms under CVI conditions, and $\simeq10^9$ atoms for a complete simulation. In Eq. (6) the time integration was carried out as a summation over time steps $\Delta t=1$ fs, while for the radius r in Eq. (1) integration was carried out by summation over discrete shells of equal widths.

IV. RESULTS

A. Intrananodroplet yields

In Figs. 1 and 2 we present the results of the calculations of the Y_{INTRA} yields, Eqs. (1) and (6), under CVI conditions, attained when only the dynamics of the bare nuclei is considered. Figure 1 portrays the neutron yields for the highly efficient $^3\mathrm{T}(d,n)^4\mathrm{He}$ reaction generated by the INTRA mode in a $(\mathrm{D}^+\mathrm{T}^+)_n$ nanodroplet [$A=$D and $B=$T in Eqs. (1)–(5)]. The energy-dependent cross sections $\sigma(E')$ were inferred from the $\sigma(E_D)$ data with the T nuclei at rest [29], being large in the high energy domain, i.e., $\sigma(E')=2\times10^{-24}-5\times10^{-24}$ cm^2, at the center of mass energies of $E'=40-140$ keV. The neutron yield per nanodroplet and per laser pulse steeply increases in the nanodroplet size domain of $R_0=1000-2000$ Å ($n=1.4\times10^8-1.0\times10^9$). For the largest nanodroplet size studied herein (Fig. 1) of $R_0=2700$ Å ($n=2.0\times10^9$), the neutron yield per nanodroplet per laser pulse is $Y_{\mathrm{INTRA}}=200$. In Fig. 2 we display the γ-ray yields for the $^{12}\mathrm{C}(p,\gamma)^{13}\mathrm{N}$ reaction generated by the INTRA mode in a $(\mathrm{C}^{6+}\mathrm{H}_4^+)_n$ nanodroplet [$A=$H and $B=$C in Eqs. (1)–(5)]. The cross sections of the resonance $^{12}\mathrm{C}(p,\gamma)^{13}\mathrm{N}$ reaction (Fig. 2) are considerably lower than those for the $^3\mathrm{T}(d,n)^{13}\mathrm{N}$ reaction (Fig. 1), reaching the maximal value of $\sigma=7\times10^{-29}$ cm^2 at $E'=425$ keV [16]. Consequently, the ratio of the INTRA yields for the $^{12}\mathrm{C}(p,\gamma)^{13}\mathrm{N}$ reaction in nanodroplets of similar sizes are expected to be considerably lower than for the $^3\mathrm{T}(d,n)^4\mathrm{He}$ reaction. Our computations (Fig. 2) demonstrate that the INTRA yields for the $^{12}\mathrm{C}(p,\gamma)^{13}\mathrm{N}$ reaction are low (Fig. 2), being $Y_{\mathrm{INTRA}}=4\times10^{-4}$ per pulse per nanodroplet for the largest $(\mathrm{CH}_4)_n$ nanodroplet studied herein, with $R_0=1790$ Å ($n=3.9\times10^8$). Y_{INTRA} for the $^{12}\mathrm{C}(p,\gamma)^{13}\mathrm{N}$ reaction (Fig. 2) increases steeply with increasing the nanodroplet size in the range $R_0=800-1300$ Å and exhibits a linear dependence on n for $R_0>1300$ ($n>1.5\times10^8$), being qualitatively similar to the pattern for the $^3\mathrm{T}(d,n)^4\mathrm{He}$ reaction (Fig. 1).

We demonstrated the occurrence of INTRA collisions and nucleosynthesis reactions driven by CE of heteronuclear nanodroplets, which satisfies the kinematic condition $\eta_{AB}>1$ (Sec. II). On the other hand, we expect that the INTRA collisions and reactions will be ineffective for the INTRA $^{12}\mathrm{C}(d,n)^{13}\mathrm{N}$ reaction driven by CE of $(\mathrm{C}^{6+}\mathrm{D}_4^+)_n$ nanodroplets, for which $\eta_{\mathrm{DC}}=1$. We performed simulations for CE and INTRA collisions of $(\mathrm{C}^{6+}\mathrm{D}_4^+)_n$ nanodroplets ($R_0=1000-1790$ Å). CE under CVI conditions provided only a minor contribution of INTRA $\mathrm{D}^+ + \mathrm{C}^{6+}$ collisions, which probably originates from the contribution of the exploding surface profile [mechanism (i) in Sec. II]. The center of mass energy of the $\mathrm{D}^+ + \mathrm{C}^{6+}$ INTRA collisions in CE of $(\mathrm{C}^{6+}\mathrm{D}_4^+)_n$ is, however, low. For example, in CE of the $(\mathrm{C}^{6+}\mathrm{D}_4^+)_n$ nanodroplet of maximal size $R_0=1790$ Å used herein, the center of mass energies of the $\mathrm{D}^+ + \mathrm{C}^{6+}$ collisions do not exceed $E'=75$ keV, as compared to high energies of up to $E'\simeq1-2$ MeV for the $\mathrm{H}^+ + \mathrm{C}^{6+}$ collisions in CE of a $(\mathrm{C}^{6+}\mathrm{H}_4^+)_n$ nanodroplet of the same size. The energy $E'=75$ keV for the $\mathrm{D}^+ + \mathrm{C}^{6+}$ collision is considerably lower than the reaction threshold $E'=500$ keV for the $^{12}\mathrm{C}(d,n)^{13}\mathrm{N}$ reaction. Thus this INTRA reaction driven by CE with $\eta_{\mathrm{CD}}=1$ is precluded. This result demonstrates that the kinematic overrun effects dominate INTRA reactions.

The laser intensity range where the Y_{INTRA} data (Figs. 1 and 2) are applicable corresponds to the CVI conditions for CE, when nanoplasma effects are minor. CVI conditions prevail in CE driven by ultrashort Gaussian laser pulses provided that complete outer ionization is accomplished prior to the attainment of the laser peak intensity [24,30]. The border radius $R_0^{(I)}$ for the CVI domain is realized for an initial nanodroplet radius of $R_0 < R_0^{(I)}$ [24,30]. The dependence of $R_0^{(I)}$ on the laser peak intensity I_M and on the pulse length τ for a Gaussian pulse is determined by $R_0^{(I)} \propto I_M^{1/2}\tau^{0.64}$ [30,31]. For superintense pulses, i.e., $I_M = 10^{20}-10^{21}$ W cm^{-2}, $R_0^{(I)}$ assumes very large values, which are comparable to R_0, and that increase with increasing τ. For CE of $(CH_4)_n$ nanodroplets driven by a Gaussian pulse at $I_M = 10^{20}$ W cm^{-2}, we estimate that $R_0^{(I)} = 750$ Å for $\tau = 25$ fs, and $R_0^{(I)} = 1820$ Å for $\tau = 100$ fs, while at $I_M = 10^{21}$ W cm^{-2} and $\tau = 25$ fs, $R_0^{(I)} = 2250$ Å [15]. Accordingly, the data for CE of $(CH_4)_n$ (Fig. 2) correspond to the CVI domain $I_M = 10^{20}$ W cm^{-2} and $\tau = 100$ fs, or $I_M = 10^{21}$ W cm^{-2} and $\tau = 25$ fs. For CE of $(DT)_n$ nanodroplets at $I_M = 10^{20}$ W cm^{-2} we estimate that $R_0^{(I)} = 1100$ Å at $\tau = 25$ fs and $R_0^{(I)} = 2670$ Å at $\tau = 100$ Å, while $R_0^{(I)} = 3300$ Å at $I_M = 10^{21}$ W cm^{-2} and $\tau = 25$ fs. The data for CE of $(DT)_n$ (Fig. 1) again correspond to the CVI domain at $I_M = 10^{20}$ W cm^{-2} and $\tau = 100$ fs or at $I_M = 10^{21}$ W cm^{-2} and $\tau = 25$ fs. The INTRA yields presented in Figs. 1 and 2 are expected to be reliable in the range $I_M = 10^{20}$ W cm^{-2}($\tau = 100$ fs)-10^{21} W cm^{-2}($\tau = 25$ fs). From this analysis we infer that at $I_M = 10^{20}$ W cm^{-2} and $\tau = 25$ fs the data of Figs. 1 and 2 correspond to $R_0 \gtrsim R_0^{(I)}$, and the INTRA yields are overestimated. Complete SEID simulations, including the contribution of the nanoplasma electrons, were performed for a near infrared laser (photon energy 1.44 eV; frequency $\nu = 0.33$ fs^{-1}) at $I_M = 10^{20}$ W cm^{-2} and $\tau = 25$ fs. For a $(CH_4)_n$ nanodroplet with $R_0 = 1800$ Å ($n = 3.9 \times 10^9$), for which $R_0/R_0^{(I)} = 2.4$, we obtained (with $s = 10^5$) $Y_{\mathrm{INTRA}} = 3.5 \times 10^{-4}$, which is lower by a numerical factor of 20% than the CVI result $Y_{\mathrm{INTRA}} = 4 \times 10^{-4}$ (Fig. 2). For the $(DT)_n$ nanodroplet with $R_0 = 1500$ Å ($R_0/R_0^{(I)} = 1.36$) we obtained (with $s = 10^5$) $Y_{\mathrm{INTRA}} = 10.3$, which is lower by a numerical factor of 2.4 than the CVI result (Fig. 1), while for $R_0 = 2700$ Å ($R_0/R_0^{(I)} = 2.45$) we obtained (with $s = 2 \times 10^5$) $Y_{\mathrm{INTRA}} = 140$, which is lower by a numerical factor of 1.4 than the CVI result. We conclude that the yield data of Figs. 1 and 2 constitute an upper limit at $I_M = 10^{20}$ W cm^{-2} ($\tau = 25$ fs) and are expected to be reliable for $I_M > 10^{20}$ W cm^{-2} at this pulse length.

B. Time-resolved dynamics of intrananodroplet nucleosynthesis

Of interest are time-resolved dynamic data for INTRA nucleosynthesis. In Fig. 3 we present the time dependence of the differential yield $y(t)$ [Eq. (1)], calculated under CVI conditions, for a $(DT)_n$ nanodroplet with $R_0 = 2030$ Å ($n = 8.15 \times 10^8$) and for a $(CH_4)_n$ nanodroplet with $R_0 = 1370$ Å ($n = 1.66 \times 10^8$). Figure 3 also shows the CE dynamics of the heavy ions that are characterized by the volume ratio $\varphi_B(t) = [R_B(0)/R_B(t)]^3$, where $R_B(t)$ is the boundary

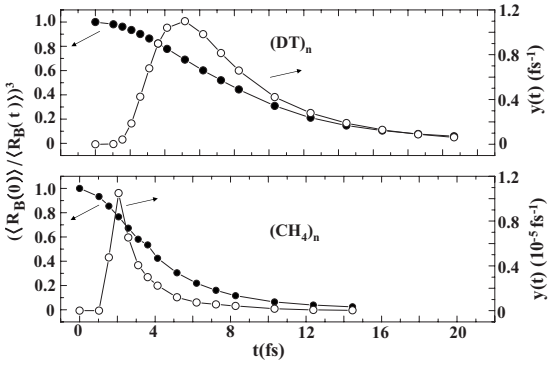

FIG. 3. Time dependence of the differential yield $y(t)$, Eq. (1), and of CE dynamics characterized by the volume ratio $[R_B(0)/R_B(t)]^3$ (see text). Calculations were performed under CVI conditions. Upper panel: Data for the intrananodroplet $^3\mathrm{T}(d,n)^4\mathrm{He}$ reaction driven by CE of $(D^+T^+)_n$. Lower panel: Data for the intrananodroplet $^{12}\mathrm{C}(p,\gamma)^{13}\mathrm{N}$ reaction driven by CE of $(C^{6+}H^+)_n$.

radius appearing in Eq. (1) and $t = 0$ marks the CE temporal onset. For both nanodroplets the time dependence of $y(t)$ (which will be referred to as the "reaction pulse") is asymmetric, manifesting a steep initial rise and a maximum followed by a slow decrease (Fig. 3). The maxima $t_{\max}$ of the FWHM Δ of the reaction pulses are $t_{\max} = 5$ fs and $\Delta = 6.6$ fs for $(DT)_n$, and $t_{\max} = 2.5$ fs and $\Delta = 1.4$ fs for $(CH_4)_n$, with the I_{INTRA} reaction time scale being shorter for $(CH_4)_n$, than for $(DT)_n$, due to more effective energetic boosting in the former case. It should be noted that the major contribution to the INTRA yield, Eq. (1), is provided when the density of nuclei is large. CE dynamics is specified by the decay time t_{CE}, defined as $\varphi(t_{\mathrm{CE}}) = 1/2$. For CE the $(CH_4)_n$ nanodroplet is characterized by $t_{\mathrm{CE}} = 4$ fs, being shorter than $t_{\mathrm{CE}} = 14$ fs for CE of the $(DT)_n$ nanodroplet. The times $t_{1/2}$ specifying the attainment of half of the total INTRA yield are $t_{1/2} = 7$ fs for $(DT)_n$ and $t_{1/2} = 2.7$ fs for $(CD_4)_n$. Accordingly, $t_{1/2} < t_{\mathrm{CE}}$ in both cases, so that INTRA nucleosynthesis occurs on a time scale shorter than CE. High average heavy ion densities at $t_{1/2}$ correspond to $\varphi(t_{1/2}) = 0.55$ for $(DT)_{8.2\times10^8}$, and $\varphi(t_{1/2}) = 0.65$ for $(CH_4)_{1.7\times10^8}$. An important characterization of the INTRA dynamics obtained from Fig. 3 is that the "reaction pulses" $y(t)$ arise almost concurrently with CE onset and are very short, being in the range of $t_{\mathrm{pulse}} \sim 5-20$ fs. These ultrashort time scales for t_{pulse} were obtained for nanodroplet sizes of $R_0 = 1400-2000$ Å. The nanodroplet size dependence of $t_{\mathrm{pulse}} \propto R_0/\tilde{v}$, where $\tilde{v}$ is a characteristic velocity of the light ions within the exploding nanodroplet, implies a near linear increase of t_{pulse} with increasing the nanodroplet size.

C. Parallel INTRA-nanodroplet and INTER-nanodroplet reactions

From the foregoing analysis we conclude that for $(DT)_n$ nanodroplets (Fig. 1) the INTRA reaction yields for nucleosynthesis is sufficiently high, i.e., $Y_{\mathrm{INTRA}} = 200$ (for $R_0 = 2700$ Å), to be amenable for experimental observation for a single nanodroplet. On the other hand, for $(CH_4)_n$ the IN-

TRA reaction yields are low, requiring experimental observation of this process from an assembly of nanodroplets. The total INTRA nucleosynthesis yield $Y_{\mathrm{INTRA}}^{\mathrm{total}}$ (per laser pulse) from an assembly containing N_{nd} nanodroplets in the laser focal volume will be

$$Y_{\mathrm{INTRA}}^{\mathrm{total}} = N_{nd} Y_{\mathrm{INTRA}} \tag{7}$$

with

$$N_{nd} = V_f \rho_{\mathrm{mol}}/n, \tag{8}$$

where ρ_{mol} is the average molecular density in the laser focal volume V_f [12] and n is the number of molecules in the nanodroplet. For INTRA yields from an assembly of $(CH_4)_n$ nanodroplets ($R_0=1000-1800$ Å and $n=6.7\times10^7-3.9\times10^8$) with $V_f=5\times10^{-7}$ cm^3 [16] and $\rho_{\mathrm{mol}}=4\times10^{18}$ cm^{-3} we estimate for $R_0=1000$ Å ($N_{nd}=3\times10^4$) that $Y_{\mathrm{INTRA}}^{\mathrm{total}}=1.4\gamma$ photons per laser pulse, while for $R_0=1800$ Å ($N_{nd}=5.1\times10^3$) $Y_{\mathrm{INTRA}}^{\mathrm{total}}=2.1\gamma$ photons per laser pulse. Accordingly, the INTRA $^{12}\mathrm{C}(p,\gamma)^{13}\mathrm{N}$ reactions driven by CE of $(CH_4)_n$ in an assembly of nanodroplets can be experimentally observed. For the efficient $^3\mathrm{T}(d,n)^4\mathrm{He}$ reaction in an assembly of $(DT)_n$ nanodroplets ($R_0=1100-2690$ Å, $n=1.4\times10^8-2\times10^9$) with $V_f=5\times10^{-7}$ cm^3 and $\rho_{\mathrm{mol}}=10^{18}$ cm^{-3}, we estimate the large total yields to be $Y_{\mathrm{INTRA}}^{\mathrm{total}}=1.2\times10^4-5.0\times10^4$ neutrons per laser pulse.

Even if the yield for INTRA reactions is sufficiently high, they have to be compared to and distinguished from the yield for the corresponding INTER reactions in a nanodroplet assembly [21]. According to our previous analysis [15,16], the major contribution to the INTER reactions originates from the outside laser filament (OF) reaction mode [15,16], with the yield Y_{INTER} per laser pulse normalized per one nanodroplet and being given by [16]

$$Y_{\mathrm{INTER}} = k_A k_B \rho_{\mathrm{mol}} \ell_{\mathrm{OF}} n \langle \sigma \rangle, \tag{9}$$

where k_A and k_B are the number of A and B atoms within a single molecular constituent, respectively, ℓ_{OF} is the reaction path length for the OF reaction mode, and $\langle\sigma\rangle$ the energy averaged cross section [16]. In Figs. 1 and 2 we also present the simulation results for the size dependence of Y_{INTER} obtained under CVI conditions with the same value of ρ_{mol} and N_{nd} as used above for the evaluation of $Y_{\mathrm{INTRA}}^{\mathrm{total}}$, Eqs. (7) and (8), and of $\ell_{\mathrm{OF}}=0.1$ cm [16].

In Fig. 1 we present the INTER reaction yield, Y_{INTER}, in an assembly of $(DT)_n$ nanodroplets, Eq. (9). Only for the lower nanodroplet size of $R_0=1100$ Å, $Y_{\mathrm{INTER}}>Y_{\mathrm{INTRA}}$. For larger nanodroplets of $R_0=1490-2690$ Å (Fig. 2), $Y_{\mathrm{INTER}}=16-27$, while $Y_{\mathrm{INTRA}}=23-204$, with Y_{INTRA} exceeding Y_{INTER} and providing the dominant reaction channel. For the INTER processes in an assembly of $(CH_4)_n$ nanodroplets, Y_{INTER} (per nanodroplet per laser pulse) manifests a weak size dependence in the range of $R_0=880-1345$ Å, where $Y_{\mathrm{INTER}}=(0.9-1.0)\times10^{-4}$. $Y_{\mathrm{INTER}}=1.0\times10^{-4}-2.9\times10^{-5}$ (Fig. 2) exhibits a decrease in the range of $R_0=1345-1790$ Å. The Y_{INTER} yields (Fig. 2) are larger than the Y_{INTRA} yields at the lower part of the size interval. For the largest nanodroplets studied herein ($R_0=1790$ Å), $Y_{\mathrm{INTER}}=2.9\times10^{-5}$, which is lower than $Y_{\mathrm{INTRA}}=4\times10^{-5}$, with a dominating contribution to nucleosynthesis originating from the INTRA mode. The total INTER reaction yields from an assembly of nanodroplets is

$$Y_{\mathrm{INTER}}^{\mathrm{total}} = N_{nd} Y_{\mathrm{INTER}}, \tag{10}$$

where Y_{INTER} is given by Eq. (9) and N_{nd} is given by Eq. (8). Equation (10) should be used for confrontation with experimental results.

It is interesting to enquire what the implications of the parallel INTRA and INTER nucleosynthesis reactions are and, in particular, whether it is possible to resolve the particle (neutrons or γ photons) emission originating from the new INTRA mechanism. For an assembly of nanodroplets, the INTRA and INTER reaction channels can be distinguished by the dependence on the density ρ_{mol} of the reaction yields for an assembly of exploding nanodroplets. The INTRA yield from an assembly of N_{nd} nanodroplets is $Y_{\mathrm{INTRA}}^{\mathrm{total}} \propto \rho_{\mathrm{mol}}$ [Eqs. (7) and (8)], while the INTER yield from such an assembly is $Y_{\mathrm{INTRA}}^{\mathrm{total}}=N_{nd}Y_{\mathrm{INTER}} \propto \rho_{\mathrm{mol}}^2$ [Eqs. (9) and (10)]. Accordingly, we expect that a study of the density dependence of the yields will provide a diagnostic tool for the identification of the INTRA process. The realization of different time scales for the INTRA and INTER processes will provide another diagnostic tool for the identification of the INTRA process. The analysis of the time-resolved dynamics of the INTRA process presented herein (Sec. IV B), together with our previous analysis of the time scale for the dominating OF contribution of the INTER processes, reveals two distinct time intervals for the two mechanisms. For the $^{12}\mathrm{C}(\mathrm{p},\gamma)^{13}\mathrm{N}$ process the γ-ray emission in the INTRA mechanism is ultrafast on the time scale of 10–15 fs (Fig. 3), while the INTER mechanism is characterized by a time scale of 2–100 ps [16]. Time-resolved γ ray emission from exploding methane nanodroplets is expected to provide new dynamic information on nucleosynthesis within a single nanodroplet. This approach is currently fraught with experimental difficulties, as will be discussed in Sec V.

V. DISCUSSION

We advanced a theoretical and computational study of intrananodroplet nuclear reactions driven by CE within a single heteronuclear $(DT)_n$ and $(CH_4)_n$ nanodroplet involving $^3\mathrm{T}(d,n)^4\mathrm{He}$ fusion and $^{12}\mathrm{C}(p,\gamma)^{13}\mathrm{N}$ nucleosynthesis. Four conclusions emerge from this analysis.

(1) The INTRA $^3\mathrm{T}(d,n)^4\mathrm{He}$ reaction yield from CE of a single, large $(DT)_n$ nanodroplet is high, i.e., $Y_{\mathrm{INTRA}}=200$ neutrons per nanodroplet per laser pulse for $R_0=2700$ Å ($n=2\times10^9$). This high yield is due to the large cross sections for this fusion reaction [29]. Accordingly, the neutron yield is sufficiently high to warrant experimental observation for a single nanodroplet. The single nanodroplet experiment can be conducted for a nanodroplet in an electromagnetic trap or for a surface deposited nanoparticle of $(DT)_n$. The surface deposited nanoparticle may assume a different structure from the spherical nanodroplet [32]. The response of a nanoparticle of different shapes to an ultraintense laser can be handled by SEID simulations.

(2) For CE of a $(CH_4)_n$ nanodroplet the INTRA $^{12}C(p,\gamma)^{13}N$ reaction yield for γ ray emission is rather low, i.e., at $R_0=1790$ Å ($n=3.9\times10^8$) $Y_{INTRA}=4\times10^{-4}$ per nanodroplet per laser pulse. Accordingly, this INTRA process is amenable to experimental observation only in an assembly of such nanodroplets, e.g., in a nanodroplet spray. Under realistic experimental conditions of $R_0=1800$ Å ($n\simeq4\times10^8$) we estimate that $Y_{INTRA}^{total}\simeq2\gamma$ rays per laser pulse.

(3) From estimates of the relative contributions for the new INTRA reaction and for the conventional INTER reaction in an assembly of nanodroplets we concluded that for the largest nanodroplets studied herein, i.e., $R_0=1490-2690$ Å ($n=3.4\times10^8-2.0\times10^9$) for $(DT)_n$ and $R_0=1790$ Å ($n=3.9\times10^8$) for $(CH_4)_n$, nucleosynthesis is dominated by the new INTRA mode. It is important to note that while INTER reaction modes for fusion and nucleosynthesis dominate in CE of heteronuclear clusters [4–7,12] and moderately small nanodroplets ($R_0\lesssim500$ Å) [16], the INTRA reaction modes dominate for the large $(DT)_n$ and $(CH_4)_n$ heteronuclear nanodroplets studied herein. Our analysis provides approaches to resolve particle (neutrons or γ rays) emissions originating from the INTRA and INTER mechanisms in an assembly of nanodroplets. A straightforward approach rests on the dependence of the yields on the molecular density ρ_{mol}. As shown in Sec. III the yields are $Y_{INTRA}^{total}\propto\rho_{mol}$ [Eqs. (7) and (8)], while $Y_{INTER}^{total}\propto\rho_{mol}^2$ [Eqs. (9) and (10)], so that the dependence of the total assembly yields on ρ_{mol} will distinguish between the new INTRA and the traditional INTER reaction modes. Time-resolved particle (neutrons or γ rays) emissions from exploding nanodroplets, which result in different time scales for the INTRA reaction (10–15 fs) and for the INTER reaction (2–100 ps), may provide a new tool for the identification of the INTRA mode. At present, sufficiently fast particle counters (with subpicosecond time resolution) are not available, hampering the application of this approach.

(4) A striking manifestation of the kinematic constraints of $\eta_{AB}>1$ for effective INTRA collisions and reactions was predicted and confirmed by SEID simulations. CE of the $(C^{6+}D_4^+)_n$ nanodroplet with $R_0=1790$ Å ($n=3.9\times10^8$) results only in low-energy collisions with $E'\leq75$ keV, in striking contrast to CE of the $(C^{6+}H_4^+)_n$ nanodroplet of the same size, which results in high-energy collisions of up to $E'\simeq1-2$ MeV. Accordingly, the INTRA $^{12}C(d,n)^{13}N$ reaction driven by INTRA CE of $(C^{6+}D_4^+)_n$ with $\eta_{DC}=1$ is precluded. This negative prediction highlights the crucial role of kinematic overrun effects in inducing INTRA heteronanodroplet nucleosynthesis.

For the $t+d$, $p+^{12}C$, and $d+^{12}C$ INTRA reactions driven by CE of $(DT)_n$, $(CH_4)_n$, and $(CD_4)_n$ nanodroplets, respectively, experimental results are not yet available. The present study provides predictions for future experimental studies of this new class of INTRA-nanodroplet dynamics.

From our analysis of CE driven INTRA nuclear reactions we assert that the characterization of an effective single nanodroplet as a target for fusion and nucleosynthesis is realized under the following intrinsic conditions:

(1) Driving of the nanodroplet by lasers of sufficient high intensity, which insures complete inner ionization of the atoms.

(2) Insuring nearly complete outer ionization, with the nanodroplet's initial radius being smaller than, or comparable to, the border radius $R_0^{(I)}$, which depends on the laser intensity and laser parameters, as well as on the charges of nuclei (ions) and on the nanostructure packing [16,24,30,31].

These two intrinsic conditions characterize the choice of the laser intensity. On the basis of our complete SEID simulations, including the contribution of the nanoplasma electrons (Sec. IV A), we assert that the INTRA yield data under CVI conditions reported herein for $(DT)_n$ and $(CH_4)_n$ nanodroplets are reliable for $I_M\gtrsim10^{20}$ W cm^{-2} (for a pulse length of $\tau=25$ fs). Such superintense pulses are currently available [33]. Even higher ultraintense laser fields of $I_M\geq10^{21}-6\times10^{22}$ W cm^{-2} were already used in a theoretical study of ionization and dissociation of muonic molecular ions [34]. The ultrahigh intensities of $I_M\gtrsim10^{20}$ W cm^{-2} for INTRA reactions may also be relevant in the context of light absorption within a single nanodroplet. A basic assumption underlying our treatment of INTRA collisions and reactions is that the laser field inside a nanodroplet is spatially homogeneous, and that there is no attenuation (due to absorption) along its propagation path inside the nanodroplet. Following our previous treatment [16,35] we consider attenuation within the nanodroplet to be unimportant if $E_{fl}>2E_{tot}$, where E_{fl} is the energy flow through the nanodroplet and E_{tot} is the total energy absorbed by nanodroplet particles (electrons and ions), which is dominated by the energy of the ions [16,35]. On the basis of our previous analysis [16,35] we considered attenuation in $(DT)_n$ and $(CH_4)_n$ nanodroplets driven by a Gaussian laser pulse with $I_M=10^{20}$ W cm^{-2} and $\tau=25$ fs. For $(DT)_n$ nanodroplets our simulations result in $E_{tot}=5.31\times10^{11}$ keV and $E_{fl}=2.60\times10^{13}$ keV (for $R_0=1100$ Å), $E_{tot}=2.49\times10^{12}$ keV and $E_{fl}=4.26\times10^{13}$ keV (for $R_0=1490$ Å), and $E_{tot}=9.69\times10^{12}$ keV and $E_{fl}=6.32\times10^{13}$ keV (for $R_0=2000$ Å). For $(CH_4)_n$ nanodroplets we obtained $E_{tot}=1.63\times10^{12}$ keV and $E_{fl}=5.83\times10^{13}$ keV (for $R_0=880$ Å), while $E_{tot}=1.21\times10^{13}$ keV and $E_{fl}=9.86\times10^{13}$ keV (for $R_0=1350$ Å). From these numerical results we conclude that at $I_M=10^{20}$ W cm^{-2} ($\tau=25$ fs) the condition $E_{fl}\gg E_{tot}$ is satisfied for the relevant nanodroplet size domain. As $E_{fl}\propto\tau I_M$ [16,34], we expect that this condition will also apply at $I_M>10^{20}$ W cm^{-2} and also for longer values of τ (>25 fs). We infer that the condition for weak attenuation is satisfied for all the nanodroplet sizes $R_0=1000-3000$ Å, with laser pulse parameters considered herein. The largest nanodroplet sizes used in our calculations become comparable to the near-infrared laser wavelength of $\lambda=860$ nm, i.e., $R_0/\lambda=0.1-0.3$. For larger nanodroplets an extension of the treatment of laser-nanodroplet will be required.

The use of an assembly of nanodroplets as a target for CE driven INTRA nucleosynthesis reactions requires that intrinsic conditions (1) and (2) will be supplemented by additional extrinsic conditions.

(3) Dependence on the average density ρ_{mol} and on the number N_{nd} of nanodroplets in the laser focal volume. As discussed above, $Y_{INTRA}^{total}\propto N_{nd}\propto\rho_{mol}$ for a nanoparticle assembly increasing linearly with increasing the density. This increase with increasing ρ_{mol} will be limited by the attenuation of the laser intensity by the assembly.

(4) Geometrical parameters of the laser focal volume. Low values of the radius and of the laser focal volume V_f, Eq. (8), are necessary to achieve the ultrahigh intensities ($I_M = 10^{20} - 10^{21}$ W cm^{-2}) required for the attainment of the INTRA reaction. For a nanodroplet assembly the low value of V_f will reduce the nanoparticle number N_{nd}, Eq. (8), and Y_{INTRA}^{total}, Eq. (7).

(5) The dimensionality of the nanodroplet assembly. Our theoretical-computational studies pertain to a three-dimensional assembly in beams or sprays. Nanoparticles deposited on surfaces will provide a two-dimensional target. This geometry will be advantageous for INTRA single nanodroplet nucleosynthesis, however, it will lead to the reduction of the effective number of particles and of the total INTRA yield for the assembly.

These intrinsic and extrinsic conditions for effective target reactions provide some guidelines for optimization of INTRA nuclear reactions within a single nanodroplet and in an assembly of nanodroplets.

We conclude with some comments on single nanodroplet dynamics, pertaining to the concept of temporal confinement and to the insight gained on the early stages of intrananodroplet CE. The INTRA reactions driven by CE within a single heteronuclear nanodroplet extend the research area of single molecule [36,37] and single protein [38,39] spectroscopy and dynamics to the realm of nanoscience, encompassing CE dynamics within a single nanostructure. The enhancement of efficient reactions within a nanodroplet requires the operation of a mechanism of particle (nuclei) confinement. However, CE results in the expansion of the nanostructure, being in apparent contradiction with the concept of confinement. An INTRA reaction driven by CE of a heteronuclear nanodroplet, which rests on kinematic overrun effects, involves a transient temporal confinement of the heavy nuclei over the fs time scale, with the heavy nuclei subcluster acting as a target for the expanding light nuclei (i.e., protons or deuterons). Up to now, experimental studies of CE focused on the kinetic energy, angular distribution, and INTER reactions of the high energy nuclei and ions interrogated at large, macroscopic distances from the initially exploding CaN [6]. The present study provides insight into the early temporal stages of CE, as interrogated by intrananodroplet collisions and reactions. These theoretical-computational results should be subjected to experimental scrutiny.

ACKNOWLEDGMENTS

We are grateful to André Bandrauk for stimulating discussions and to Fabio Peano for useful comments on the manuscript. This research was supported in part by the James Franck Binational German-Israeli Program in Laser-Matter Interaction. J.J. is grateful to the Humboldt Foundation for the support of this research during his visit to the Humboldt University of Berlin and to the Free University of Berlin.

[1] V. P. Krainov and M. B. Smirnov, Phys. Rep. **370**, 237 (2002).
[2] U. Saalmann, Ch. Siedschlag, and J. M. Rost, J. Phys. B **39**, R39 (2006).
[3] A. Heidenreich, I. Last, and J. Jortner, in *Analysis and Control of Ultrafast Photoinduced Reactions*, edited by O. Kühn and L. Wöste, Springer Series in Chemical Physics Vol. 87 (Springer, New York, 2007), p. 575.
[4] G. Grillon, Ph. Balcou, J.-P. Chambaret, D. Hulin, J. Martino, S. Moustaizis, L. Notebaert, M. Pittman, Th. Pussieux, A. Rousse, J.-Ph. Rousseau, S. Sebban, O. Sublemontier, and M. Schmidt, Phys. Rev. Lett. **89**, 065005 (2002).
[5] K. W. Madison, P. K. Patel, D. Price, A. Edens, M. Allen, T. E. Cowan, J. Zweiback, and T. Ditmire, Phys. Plasmas **11**, 270 (2004).
[6] M. Hohenberger, D. R. Symes, K. W. Madison, A. Sumeruk, G. Dyer, A. Edens, W. Grigsby, G. Hays, M. Teichmann, and T. Ditmire, Phys. Rev. Lett. **95**, 195003 (2005).
[7] S. Ter-Averisyan, M. Schnürer, D. Hilscher, U. Jahnke, S. Busch, P. V. Nickles, and W. Sandner, Phys. Plasmas **12**, 012702 (2005).
[8] T. Ditmire, J. W. G. Tisch, E. Springate, M. B. Mason, N. Hay, R. A. Smith, J. Marangos, and M. H. R. Hutchinson, Nature (London) **386**, 54 (1997).
[9] M. Lezius, S. Dobosz, D. Normand, and M. Schmidt, Phys. Rev. Lett. **80**, 261 (1998).
[10] M. Schnürer, S. Ter-Avetisyan, H. Stiel, U. Vogt, W. Radloff, M. Kalashnikov, W. Sandern, and P. V. Nickles, Eur. Phys. J. D **14**, 331 (2001).
[11] S. Fukuda, K. Yamakawa, Y. Akahane, M. Aoyama, N. Inoue, H. Ueda, and Y. Kishimoto, Phys. Rev. A **67**, 061201 (2003).
[12] J. Zweiback, R. A. Smith, T. E. Cowak, G. Hays, K. B. Wharton, V. P. Yanovsky, and T. Ditmire, Phys. Rev. Lett. **84**, 2634 (2000).
[13] M. Schnürer, S. Ter-Avetisyan, P. V. Nickles, and A. A. Andreev, Phys. Plasmas **14**, 033101 (2007).
[14] O. Karsch, S. Düsterer, H. Schwoerer, F. Ewald, D. Habs, M. Hegelich, G. Pretzler, and A. Pukho, Phys. Rev. Lett. **91**, 015001 (2003).
[15] I. Last and J. Jortner, Phys. Rev. Lett. **97**, 173401 (2006).
[16] I. Last and J. Jortner, Phys. Plasmas **14**, 123102 (2007).
[17] I. Last and J. Jortner, Phys. Rev. A **64**, 063201 (2001).
[18] I. Last and J. Jortner, J. Phys. Chem. A **106**, 10877 (2002).
[19] I. Last and J. Jortner, Phys. Rev. A **71**, 063204 (2005).
[20] A. E. Kaplan, B. Y. Dubetski, and P. L. Shkolnikov, Phys. Rev. Lett. **91**, 143401 (2003).
[21] F. Peano, J. L. Martins, R. A. Fonseca, L. O. Silva, G. Coppa, F. Peinetti, and R. Mulas, Phys. Plasmas **14**, 056704 (2007).
[22] F. Peano, R. A. Fonseca, J. L. Martins, and L. O. Silva, Phys. Rev. A **73**, 053202 (2006).
[23] H. Li, J. Liu, Ch. Wang, G. Ni, Ch. J. Kim, R. Li, and Zh. Xu, J. Phys. B **40**, 3941 (2007).
[24] I. Last and J. Jortner, J. Chem. Phys. **121**, 3030 (2004).
[25] Ch. Siedschlag and J. M. Rost, Phys. Rev. A **67**, 013404 (2003).

[26] I. Last and J. Jortner, J. Chem. Phys. **120**, 1336 (2004).
[27] G. M. Petrov, J. Davis, A. L. Velikovich, P. Keppler, D. Gasgupta, and R. W. Clark, Phys. Plasmas **12**, 063103 (2005).
[28] I. Last and J. Jortner, Phys. Rev. A **75**, 042507 (2007).
[29] D. J. Rose and M. Clark, Jr., *Plasmas and Controlled Fusion* (MIT, Cambridge, MA, 1961).
[30] I. Last and J. Jortner, Phys. Rev. A **73**, 013202 (2006).
[31] A. Heidenreich, I. Last, and J. Jortner, Eur. Phys. J. D **46**, 195 (2008).
[32] A. Lando, N. Kébaili, Ph. Cahuzac, A. Masson, and C. Bréchignac, Phys. Rev. Lett. **97**, 133402 (2006).
[33] G. A. Mourou, T. Tajima, and S. V. Bulanov, Rev. Mod. Phys. **78**, 309 (2006).
[34] S. Chelkowski, A. D. Bandrauk, and P. B. Corkum, Phys. Rev. Lett. **93**, 083602 (2004).
[35] I. Last and J. Jortner, Phys. Rev. A **73**, 063201 (2006).
[36] W. E. Moerner and M. Orrit, Science **283**, 1670 (1999).
[37] E. Barkai, Y. Yung, and R. Silbey, Annu. Rev. Phys. Chem. **55**, 457 (2004).
[38] H. Lu, L. Xun, and X. S. Xie, Science **282**, 1877 (1998).
[39] O. Flomenbom, K. Velonia, D. Loos, S. Mauo, M. Cotler, Y. Engelborghs, J. Hofkens, A. E. Rowan, R. J. M. Nolte, M. van der Auweraer, F. C. De Schrijver, and J. Klafter, Proc. Natl. Acad. Sci. U.S.A. **102**, 2368 (2005).